crystals

MDPI

Article

Flexible Optically Rewritable Electronic Paper

Vladimir Chigrinov [1,2], Aleksey Kudreyko [3,*] and Jiatong Sun [4]

[1] Department of Electronic and Computer Engineering, Hong Kong University of Science and Technology, Clear Water Bay, Kowloon, Hong Kong 999077, China; eechigr@ust.hk
[2] Nanjing Jingcui Optical Technology Co., Ltd., Nanjing 211135, China
[3] Department of General Physics, Ufa University of Science and Technology, Ufa 450076, Russia
[4] College of Information Science and Technology, Donghua University, Shanghai 201620, China; jsun@dhu.edu.cn
* Correspondence: alexkudreyko@mail.ru

Abstract: In this article, we present the procedure of preparation of flexible electronic paper with a photosensitive azo dye layer as the key element for changing the orientation of the polarization plane. The main steps of the technology for the fabrication of flexible e-paper are reported. The possible production of Digital Mirror Devices and the roll-to-roll process is discussed. Images on flexible e-paper are demonstrated, including bank card options. The advantages of optically rewritable e-paper technology in comparison with the e-ink usually used for this purpose are highlighted. Potential applications of flexible optically rewritable e-paper include price tags for supermarkets, indoor and outdoor advertisements, smart card labels, etc.

Keywords: azo dye; flexible substrates; nematic liquid crystal; optically rewritable electronic paper; photoalignment

Citation: Chigrinov, V.; Kudreyko, A.; Sun, J. Flexible Optically Rewritable Electronic Paper. *Crystals* **2023**, *13*, 1283. https://doi.org/10.3390/cryst13081283

Academic Editor: Jagdish K. Vij

Received: 31 July 2023
Revised: 13 August 2023
Accepted: 17 August 2023
Published: 20 August 2023

1. Introduction

Plastic substrates have only 1/6 of the weight of glass substrates. They are virtually unbreakable, their flexibility allows them to be shaped other than in planar displays and the display is thinner, which provides a wider viewing angle. These properties render them attractive for portable liquid crystal devices. However, a series of problems regarding cell gap control and alignment of liquid crystals on a flexible substrate required new technical solutions.

Photoalignment of nematic liquid crystals (NLC) represents an emerging technology for the production of liquid crystal devices with novel properties, e.g., lenses, reconfigurable optical networks, index-tunable antireflective coatings and optically rewritable phase gratings [1]. One of these devices is flexible optically rewritable electronic paper (ORW e-paper), which is a reflective display with a photosensitive substrate coated by an azo dye layer with a thickness of 10–15 nm [2–11]. This display technology has gained significant attention from scholars due to its light weight, low cost, small thickness and easy processing [12–15]. A shining example of the recent application of liquid crystals with photoalignment technology is the ProMotion display technology, used in iPad Pro displays [16].

Photoalignment of liquid crystals (LCs) has obvious advantages over substrate-rubbing technology due to its application on curved and flexible substrates, high resolution and absence of mechanical damage on the surface. Nanosized photoaligning layers are very good materials for implementation of flexible ORW e-paper [10], since the photoaligning films are robust and possess rather good LC aligning properties with sufficiently high anchoring energies, image sticking and voltage holding ratios. Another advantage of photoalignment technology for e-paper is its thermal stability up to 100 °C. Thus, photopatterning techniques, mechanical flexibility characteristics, thermally stable birefringence characteristics enabled us to fabricate flexible and lightweight color patterns.

Meanwhile, control of uniformity of the cell gap for flexible ORW e-paper remains a challenging problem. A solution to this problem was found in photoenforced stratification in the fabrication of encapsulated LC on flexible substrates [17]. Enhancement of light reflectance coefficient and optical compensation of phase retardation by plastic substrates is another important issue in the production of flexible LC displays [18]. Roller and ink-jet printers are capable of printing adhesive spacers onto a substrate [19]. However, the methods are not widely used because the equipment for LC orientation on flexible substrates is limited [10].

In order to achieve uniformity of the cell gap, we examine a method that allows fabrication of uniformly distributed spacers. In particular, we propose a technique of silicon stamping for cell gap control [5]. We established highly reliable flexible ORW e-paper without any visible change in the optical performance by optimizing the height of the spacers, their variation, the distance between them and the substrate materials. Furthermore, we show the advantages of ORW e-paper devices over electronic ink technology [20] as well as e-paper preparation by using Digital Mirror Devices (DMD) and the roll-to-roll process. We show the optical properties of flexible ORW e-paper and discuss possible applications for indoor and outdoor imaging. An image of the ORW e-paper on a smart card is presented.

Future research into flexible ORW e-paper should be devoted to investigation of the following: (i) full color with a wide color triangle; (ii) effective outdoor performance in direct sunlight; (iii) further optimization of photoalignment azo dye materials and LCs used for the purpose with a high stability and fast writing/erasing time. We foresee possible applications of flexible ORW e-paper in the following: (i) indoor and outdoor sign and advertising labels; (ii) price labels in supermarkets; (iii) displays on flexible cards; (iv) conference labels; (v) personal digital assistants (PDAs).

2. Methodology of Uniform Spacer Distribution

Exposure of the surface to plane-polarized light induces in-plane rotation of azo dye molecules (chemical compound sulfonic dye known as SD1) due to interaction between dipole moments and plane-polarized light (450 $\pm$ 10 nm). It should be noted that absorption oscillator of SD1 molecules coincides with its long molecular axis. As a result, molecules absorb exposure energy for in-plane rotation, hence, long molecular axes of SD1 tend to align perpendicular to the polarization plane. When NLCs are sandwiched between the substrates, the photosensitive layer changes the director twist angle ($0 \leq \phi \leq 90^{\circ}$) across the cell, realizing a number of intermediate gray scales in the ORW e-paper (see Figure 1a). Here the thickness of the NLC layer should be high enough to set the "waveguide" regime when the polarization of the light directly follows the average orientation of the LC molecules (LC director).

The uniform thickness of the LC film plays a key role in the formation of high image quality on flexible ORW e-paper. The uniform arrangement of cylindrical pillars on the surface is the obvious way to control the cell gap [10] (see Figure 1b).

There exist two main conditions for acceptable deformation of the cell with thin flexible substrates, offering its "figure of merit" [21]:

(a) Relative compression of the spacers caused by external pressure on the first of the plates must not exceed the maximum value;

$$\frac{\Delta h}{h} = \frac{P}{sE} \leq \frac{\Delta h}{h}\text{max}.$$

(b) Maximum deflection of the top plate between the spacers must be kept within predetermined limits

$$\frac{\Delta d}{d} = \frac{PL^4}{4E_p b^3 d} \leq \frac{\Delta d}{d}\text{max},$$

where P denotes the applied external pressure to the top plate; E is the elasticity modulus of the spacers; s is the coefficient of the surface coverage by spacers; d

is the thickness of the LC layer; Δd is the maximum deflection of the plate; L is the distance between spacers, E_p is the elasticity modulus of the plate and b is the plate thickness. Conditions (a) and (b) allow measuring the external pressure for acceptable deformation.

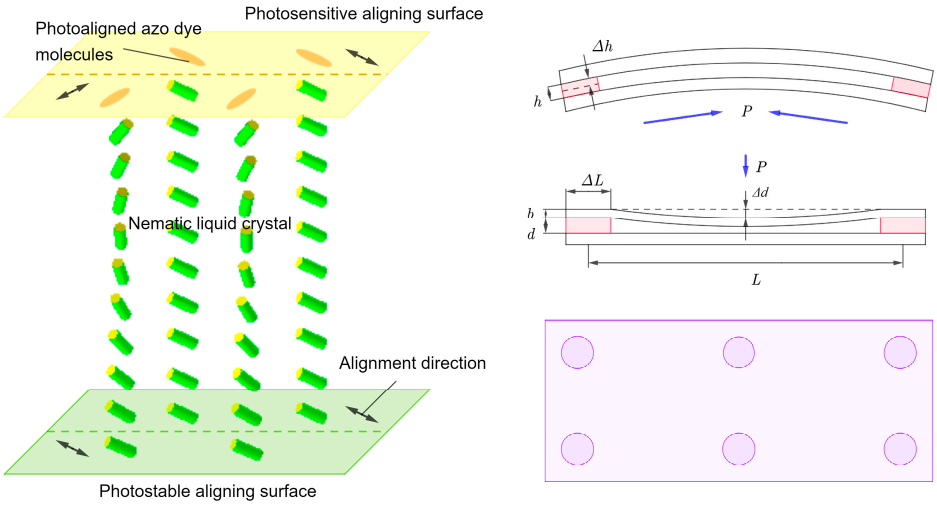

(**a**) (**b**)

Figure 1. Structure of flexible e-paper spacers: (**a**) lateral (**up**) and top (**bottom**) views; (**b**) photo-induced in-plane rotation of NLC structure by azo dye nanolayer.

In order to produce a uniform thickness layer, it is necessary to distribute the spacers on a plastic substrate. The corresponding stamping process includes the following steps: the printing roller covers the surface with printing ink, then curing with ultraviolet radiation under heating is applied to the substrate, resulting in photopolymerization of the material (see Figure 2a). Heating up to 75 °C produces strong adhesion of the spacer to the substrate. As a result, the adhesive surface layer of the spacer does not cause any leak or contamination of the LC. In the next step, the photoalignment layer (SD1) needs to be spin-coated on the substrate. The optimal thickness of the layer is about 10–15 nm. After creating the initial alignment direction on the polyethersulfone (PET) substrate and setting the alignment direction on another substrate, the surfaces are assembled together and bonded with epoxy to seal the LC cell. Clamping the silicone stamp creates a gap on the plastic substrate with a height of about 10 µm. The accuracy of the thickness between the substrates plays a minor role due to a waveguide mode. Using UV light to cure the epoxy, the spacers become solid. Another plastic substrate with a polarizer on the reverse side is coated with the alignment layer, i.e., HPL008 (DIC, Tokyo, Japan), which is not photosensitive (see Figure 1a). The flowchart of the process is shown in Figure 2b.

The microphotographs depicted in Figure 2c,d show the top view of two LC alignment structures. The image in Figure 2c appears dark due to the planar alignment of the LCs and crossed polarizers. It can be seen that the arrangement of spacers is fairly uniform. In practice, typical values of the distance between spacers L range within 60–200 µm and ΔL ranges between 5 and 25 µm, while the optimal value of $L/\Delta L = 10$. This means that the spacers cannot be directly observed by the human eye.

Following the flowchart depicted in Figure 2b, we applied the stamp printing method for the fabrication of flexible ORW e-paper. Application of this technique provides regularly distributed spacers on PET substrate. After providing the initial alignment direction on the first substrate and fixing the alignment direction on the second substrate, the two substrates were bonded together with epoxy resin. The obtained cell was filled in with NLC mixture. After exposing the cell, the desired image is obtained.

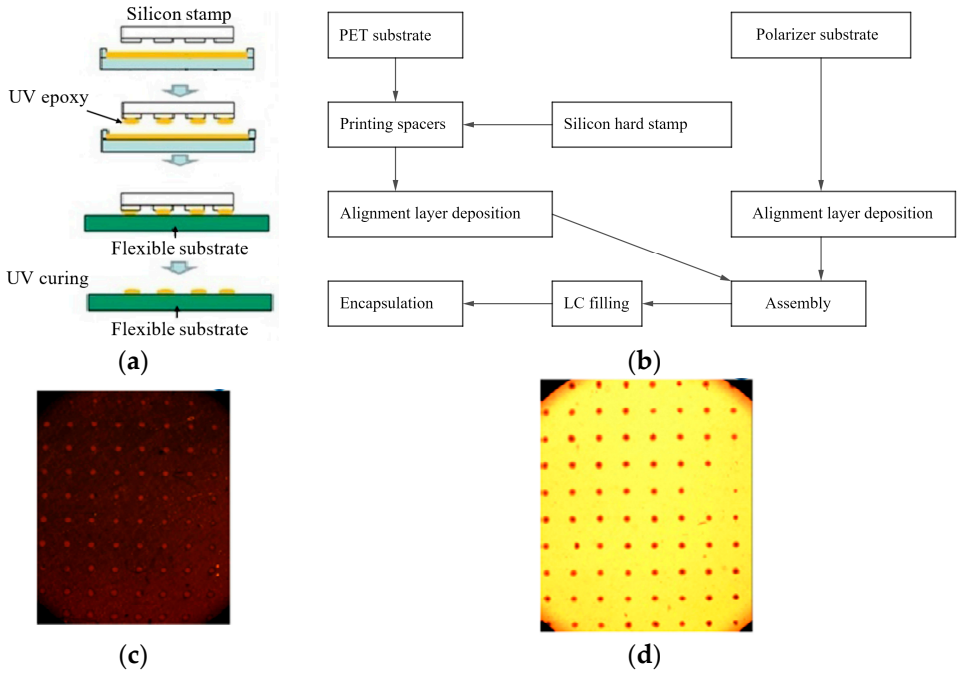

Figure 2. Color online. (**a**) Process of spacer printing. (**b**) Flowchart of the manufacturing process of flexible optically rewritable electronic paper. Microphotographs of (**c**) planar and (**d**) twisted NLC orientations. Cylindrical spacer diameter: ΔL = 20 μm; distance between spacers: L = 200 μm.

3. Results and Discussion

The image obtained in flexible ORW e-paper using the proposed technological process is clear and has good quality, illustrating the uniformity of the cell gap (Figure 3). Moreover, photoalignment of liquid crystals by azo dyes on substrates does not require high temperature, i.e., any plastic substrates can be used.

Figure 3. Sample images showing flexibility of ORW e-paper.

Experimental investigation demonstrates that there is no visible difference between flat and curved substrates. The contrast ratio superiors 30:1 and 7:1 for reflective and transmissive modes, respectively. Every transmission level is stable and visualizes information with zero power consumption for a long time. In view of the experimental results, we claim that this method is the most suitable for mass production.

Other recorded images on the ORW e-paper are shown in Figure 4. In the case of the waveguide mode ($\Delta nd/\lambda >> 1$, where Δn is the birefringence of the layer and λ the wavelength of light), the polarization of light exactly follows NLC director orientation, which is twisted to the rotation angle φ. Thus, crossed and parallel polarizers enable the observation of different images (Figure 4, right). An example of image recording process on glass plate is shown in the supplementary video.

Figure 4. ORW e-paper image showing grayscales. **Left**: Image with a resolution of 140 ppi. **Right**: two images of ORW e-paper with crossed and parallel polarizers.

Gray levels of e-paper depend on the twist angle and achieve 5 bits (see Figure 5a). The angular dependence of the contrast ratio and reflectance are shown in Figure 5b [8,22]. The results shown are compatible with other e-papers used for the purpose of imaging with zero or very small power consumption.

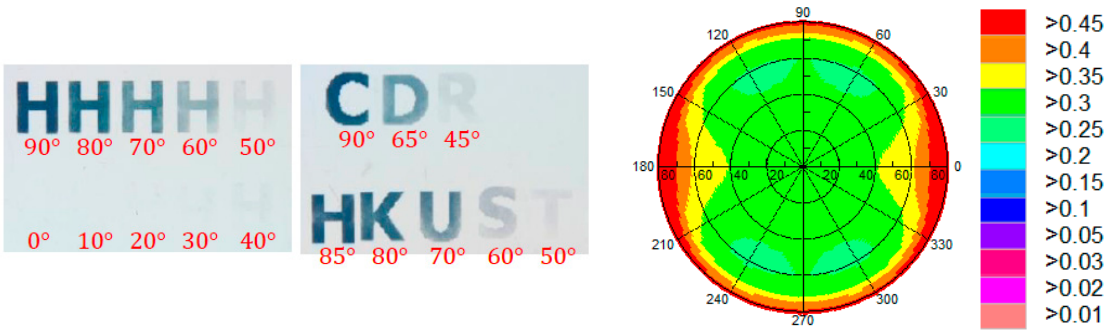

(**a**) (**b**)

Figure 5. Color online. (**a**) Grey levels of ORW e-paper, based on the rotation angle of twisted NLC layer; (**b**) angular dependence of the ORW reflectance coefficient.

The erasing and writing time of the ORW e-paper depends on the method of making the image (amplitude modulation or direct rotation of the polarized light), and usually takes several seconds, depending on the parameters of the NLCs, such as rotation, viscosity and twist elastic coefficient. Making the switching faster is not advisable, as the number of writing–erasing cycles can drastically decrease due to the change in the azo dye photoaligned NLC director orientation from planar to homeotropic.

Optically rewritable technology boasts several advantages over electronic ink, which is also used for e-paper: (i) a resolution up to 2000 ppi; (ii) it does not require a thin-film transistor and driving electronics inside the cell, it is cost-effective, and there is no issue with aperture ratio; (iii) the color triangle is better >25% NTSC, and has a high color depth (5 bits of gray levels achieved); (iv) it has a high contrast up to 30:1 in the reflective case; (v) it has an operating temperature −20–80 °C; (vi) its speed is around 1 s; (vii) it is flexible.

Let us highlight several applications of ORW technology. The concept of ORW e-paper can be extended to e-paper-based smart card (see Figure 6). Here, a LC mixture MLC-6809-000 (Merck, Germany) with an 8 μm cell gap was used as the birefringent media.

Figure 6. Color online. Prototype of ORW e-paper technology for a smart card.

After 1000 cycles of dynamic and torsional bending cyclic tests, we did not observe any visible changes in the alignment quality, cell gap or optical properties of the smart card.

Optimization of light printer parameters (wavelength of exposure, photoaligning material and divergence angle of the beam) enabled us to reduce exposure energy from $\approx$1 J/cm^2 to ($\approx$150 mJ/cm^2). These studies enabled us to use roll-to-roll technology for the production of full-color ORW e-paper devices (see Figure 7) [23,24]. A challenge for substrate transport is ensuring precise movement of the substrate.

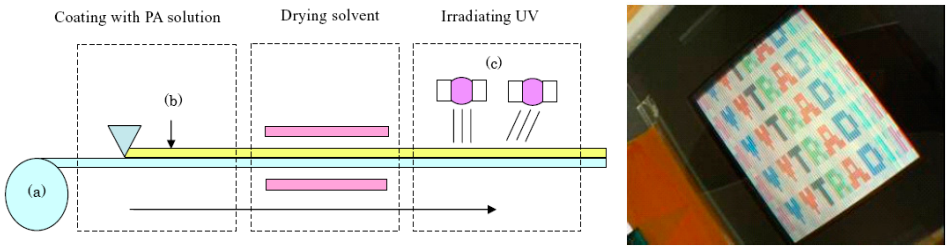

Figure 7. Color online. ORW roll-to-roll technology using azo dye photoalignment layers.

The images of ORW e-paper obtained by azo dye photoalignment technology show the following: (i) a simple configuration and cost efficiency; (ii) a high transmittance and high beam quality; (iii) a broad wavelength tolerance from vis to THz; (iv) it is reconfigurable and reusable; (v) a flexible design and new properties; (vi) a high light damage threshold.

Achieving pure phase modulation has many practical applications, e.g., modern digital and electronic technologies are based on photolithography processes. Currently developing virtual and augmented reality technologies are based on phase modulators with limited performance. Phase modulation depth and modulation rate are the most important characteristics. The characteristics also include an option of fabricating individual modulators into a dense array. The best approach to obtain pure phase modulation is to use mirrors.

In order to make polarization holography on SD1 layer, a DMD-based micro-lithography setup is suggested. The desired pattern is developed due to the reflectance of the collimated light beam from a DMD [25]. After being focused by a tunable objective, the beam is polarized by a motorized rotating polarizer and then projected onto the LC cell. A charge-coupled device (CCD) is utilized to monitor the focusing process. Consequently, a photo-patterned LC structure can be obtained. See the experimental setup for polarization imaging measurement in Figure 8.

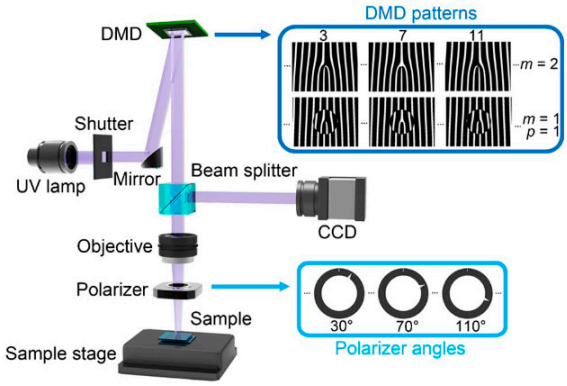

Figure 8. Color online. Digital micro-mirror device photolithography setup; m and p denote topological charge and radial index, respectively.

There exist several methods for the formation of optical vortices. The most common method is the transmission of a light beam with a predetermined Gaussian beam through an optical element with changing thickness, which forms a singularity. This element was suggested in [26] and is known as a helical phase plate.

One can observe that specially developed computer holograms convert Gaussian laser beams into the desired helical mode. The combination of photoalignment and the DMD system results in control of the LC director [27]. The obtained holograms comprise forked diffraction grating with dislocations (see Figure 9). When the polarization direction of excitation light is parallel to the alignment of LCs, the emission intensity is at its maximum (bright). At the same time, the emission intensity is at its minimum (dark) when those are perpendicular.

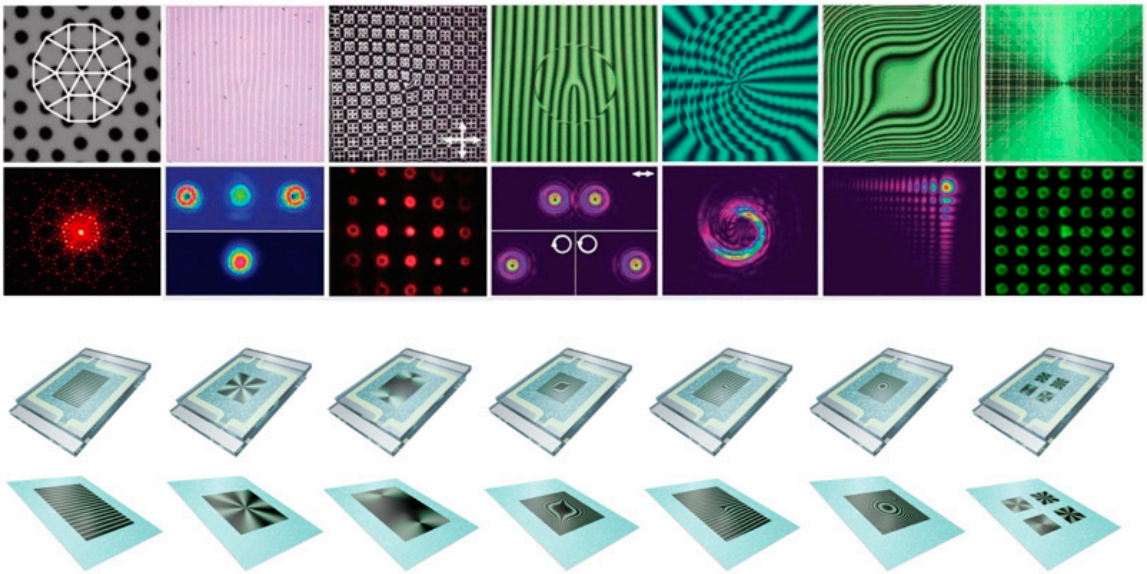

Figure 9. Color online. Recorded ORW images on DMD. Top row: CCD images captured with a phase-contrast microscope that is looking at light reflected off the surface of a phase modulator. Middle row: diffraction patterns of the samples (arrows indicate twist direction of the vortex). Bottom (blue) rows: computer-generated hologram plots.

The above images demonstrate LC fork gratings for various alignment modes with arbitrary set topological charges through photopatterning. These fork gratings exhibit high alignment quality and excellent phase retardance uniformity, as well as other advantages such as easy fabrication, simple configuration, high resolution, light weight and low cost. Optical vortices generated from these fork gratings reveal high efficiency, wide operating spectrum range, and excellent polarization independency.

4. Conclusions

A series of our research studies developed an approach to deal with flexible substrates. Flexible optically rewritable e-paper may successfully compete with other e-paper technologies, including electronic ink. We have shown a reliable method of flexible e-paper production by optimizing the height and the variation of the sticky spacers, the distance between the spacers as well as proper materials for the spacers and flexible substrates. We have shown that ORW e-paper has certain advantages over the e-ink usually used for this purpose, and demonstrated the quality of e-paper images. The possible production of flexible ORW e-paper was shown using the DMD and roll-to-roll processes. The images on flexible e-paper were demonstrated on a smart card. Potential applications of flexible ORW e-paper include price labels in supermarkets, indoor and outdoor advertisements, conference labels, etc.

Supplementary Materials: The following supporting information can be downloaded at: https://www.youtube.com/watch?v=X5CDHf4H3pY&feature=youtu.be (accessed on 18 August 2023).

Author Contributions: V.C. and A.K. designed the study and wrote the manuscript. J.S. contributed to data interpretation and suggested the material parameters, which were used for the analysis. All authors have read and agreed to the published version of the manuscript.

Funding: The results shown in this paper were supported by the State Key Lab of Hong Kong University of Science and Technology (grants nos.: FSGRF13EG35/FSGRF12EG09) and Russian Science Foundation (grant no. 20-19-00201).

Data Availability Statement: Not applicable.

Acknowledgments: V.C. and J.S. congratulate the State Key Lab of Hong Kong University of Science and Technology on its 10th Anniversary (September 2023) and grateful for fruitful collaboration with the State Key Lab members.

Conflicts of Interest: The authors declare no conflict of interest.

References

1. Quiroga, J.A.; Canga, I.; Alonso, J.; Crespo, D. Reversible photoalignment of Liquid crystals: A path toward the creation of Rewritable Lenses. *Sci. Rep.* **2020**, *10*, 5739. [CrossRef] [PubMed]
2. Wei, Y.; Chen, J.; Wang, J.; Li, X.; Zeng, H. Micro-patterned photoalignment of CsPbBr3 nanowires with liquid crystal molecule composite film for polarized emission. *Nanoscale* **2021**, *13*, 14980–14986. [CrossRef] [PubMed]
3. Geng, Y.; Yao, L.S. Effect of azimuthal anchoring energy on rewriting speed of optical rewritable e-paper. *Liq. Cryst.* **2021**, *48*, 915–921. [CrossRef]
4. Fuh, A.Y.G.; Lin, T.H.; Jau, H.C.; Hung, S.Y.; Fuh, H.R. *Optically Rewritable Reflective Liquid Crystal Display. SID Symposium Digest of Technical Papers*; Blackwell Publishing Ltd.: Oxford, UK, 2006. [CrossRef]
5. Zhang, Y.; Sun, J.; Liu, Y.; Shang, J.; Liu, H.; Liu, H.; Gong, X.; Chigrinov, V.; Kowk, H.S. A flexible optically re-writable color liquid crystal display. *Appl. Phys. Lett.* **2018**, *112*, 131902. [CrossRef]
6. Sivaranjini, B.; Mohana, K.; Esakkimuthu, S.; Ganesh, V.; Umadevi, S. Photo-responsive azo-functionalised flexible polymer substrate for liquid crystal alignment. *Liq. Cryst.* **2020**, *47*, 1354–1365. [CrossRef]
7. Weng, S.-C.; Fuh, A.Y.-G.; Tang, F.-C.; Cheng, K.T. Effect of surface condition on liquid crystal photoalignment by light-induced azo dye adsorption phenomena. *Liq. Cryst.* **2016**, *2016. 43*, 1221–1229. [CrossRef]
8. Chigrinov, V.G.; Kudreyko, A.A. Tunable optical properties for ORW e-paper. *Liq. Cryst.* **2021**, *48*, 1073–1077. [CrossRef]
9. Wu, Y.; Yang, Y.; Li, T.; Huang, S.; Huang, H.; Wen, S. Stretchable and foldable waveplate based on liquid crystal polymer. *Appl. Phys. Lett.* **2020**, *28*, 117. [CrossRef]
10. Kudreyko, A.; Chigrinov, V. Structural and Optical Characteristics of Flexible Optically Rewritable Electronic Paper. *Crystals* **2022**, *12*, 1149. [CrossRef]
11. He, Y.; Li, J.; Li, J.; Zhu, C.; Guo, J. Photoinduced dual-mode luminescent patterns in dicyanostilbene-based liquid crystal polymer films for anticounterfeiting application. *ACS Appl. Polym. Mater.* **2019**, *1*, 746–754. [CrossRef]
12. Heikenfeld, J.; Drzaic, P.; Yeo, J.S.; Koch, T. A critical review of the present and future prospects for electronic paper. *J. Soc. Inf. Display* **2011**, *19*, 129–156. [CrossRef]
13. Sivaranjini, B.; Mangaiyarkarasi, R.; Ganesh, V.; Umadevi, S. Vertical alignment of liquid crystals over a functionalized flexible substrate. *Sci. Rep.* **2018**, *8*, 8891. [CrossRef] [PubMed]
14. Lee, Y.; Kim, W.; Lee, J.H.; Kim, Y.M.; Yun, M.H. Understanding the Relationship between User's Subjective Feeling and the Degree of Side Curvature in Smartphone. *Appl. Sci.* **2020**, *10*, 3320. [CrossRef]

15. Sivaranjini, B.; Ganesh, V.; Umadevi, S. Bent-core liquid crystal-functionalised flexible polymer substrates for liquid crystal alignment. *Liq. Cryst.* **2020**, *47*, 838–850. [CrossRef]
16. Display Industry Awards: SID; 2018 [Cited 2023]. Available online: https://www.sid.org/Awards/Display-Industry-Awards (accessed on 18 August 2023).
17. Khandelwal, H.; van Heeswijk, E.P.; Schenning, A.P.; Debije, M.G. Paintable temperature-responsive cholesteric liquid crystal reflectors encapsulated on a single flexible polymer substrate. *J. Mater. Chem. C* **2019**, *7*, 7395–7398. [CrossRef]
18. Ishinabe, T.; Fujikake, H. *Optical design of flexible liquid crystal displays. High Quality Liquid Crystal Displays and Smart Devices*; Institution of Engineering and Technology: London, UK, 2019; pp. 207–222. [CrossRef]
19. Maruyama, N.; Kumashiro, Y.; Yamamoto, K. Development of cell gap spacer in LCD for ink-jet printing. Proceedings of 2008 2nd Electronics System-Integration Technology Conference, Greenwich, UK, 1–4 September 2008; IEEE: New York, NY, USA, 2008; pp. 985–988. [CrossRef]
20. Yang, B.-R. *E-Paper Displays*; John Wiley & Sons: Hoboken, NJ, USA, 2022.
21. Lagerwall, S.T.; Muravski, A.A.; Yakovenko, S.Y.; Konovalov, V.A.; Minko, A.A.; Tsarev, V.P. Pressure-Insensitive Liquid Crystal Cell. U.S. Patent no. US6184967B1, 6 February 2001.
22. Kudreyko, A.; Chigrinov, V. Optimization of image writer modes for optically rewritable electronic paper. *Liq. Cryst.* **2022**, *49*, 436–441. [CrossRef]
23. Sonehara, A.; Maruyama, K.; Ono, Y.; Sugizaki, A.; Eguchi, T.; Suzuki, Y.; Ito, T.; Kumano, A.; Takahashi, T. Continuous Coating of Photo-Alignment Layer on a Flexible Color Filter for LCDs Using a Roll-to-Roll Manufacturing Process. *SID Symp. Dig. Tech. Pap.* **2006**, *37*, 1579–1582. [CrossRef]
24. Gregg, A.; York, L.; Strnad, M. Roll-to-Roll Manufacturing of Flexible Displays. In *Flexible Flat Panel Displays*; John Wiley & Sons: The Atrium, Southern Gate, UK, 2005; pp. 409–445. [CrossRef]
25. He, G.; Sun, P.; Zhang, S.; Liu, X.; Shen, D.; Zheng, Z.G. Tunable holography with independent transflective information channels enabled by interleaved soft materials. *Opt. Mater.* **2023**, *142*, 113972. [CrossRef]
26. Oemrawsingh, S.; Van Houwelingen, J.; Eliel, E.; Woerdman, J.; Verstegen, E.; Kloosterboer, J. Production and characterization of spiral phase plates for optical wavelengths. *Appl. Optics.* **2004**, *43*, 688–694. [CrossRef] [PubMed]
27. Folwill, Y.; Zeitouny, Z.; Lall, J.; Zappe, H. A practical guide to versatile photoalignment of azobenzenes. *Liq. Cryst.* **2021**, *48*, 862–872. [CrossRef]